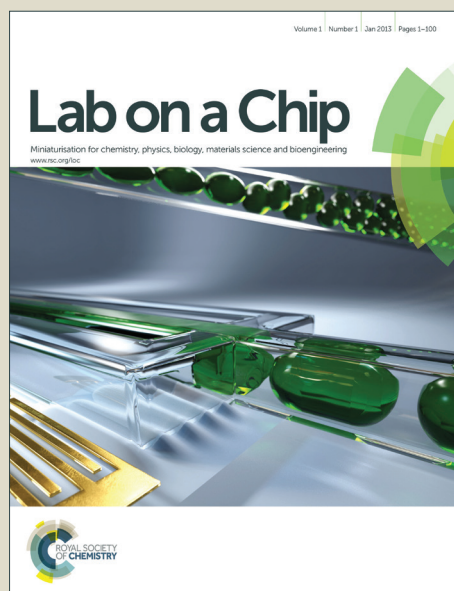


Lab on a Chip

Accepted Manuscript



This is an *Accepted Manuscript*, which has been through the Royal Society of Chemistry peer review process and has been accepted for publication.

Accepted Manuscripts are published online shortly after acceptance, before technical editing, formatting and proof reading. Using this free service, authors can make their results available to the community, in citable form, before we publish the edited article. We will replace this *Accepted Manuscript* with the edited and formatted *Advance Article* as soon as it is available.

You can find more information about *Accepted Manuscripts* in the [Information for Authors](#).

Please note that technical editing may introduce minor changes to the text and/or graphics, which may alter content. The journal's standard [Terms & Conditions](#) and the [Ethical guidelines](#) still apply. In no event shall the Royal Society of Chemistry be held responsible for any errors or omissions in this *Accepted Manuscript* or any consequences arising from the use of any information it contains.

Cite this: DOI: 10.1039/c0xx00000x

www.rsc.org/xxxxxx

ARTICLE TYPE

Nanofluidic direct formic acid fuel cell with combined flow-through and air-breathing electrode for high performance

E. Ortiz-Ortega,^a Marc-Antoni Goulet,^b Jin Wook Lee,^c M. Guerra-Balcázar,^a N. Arjona,^d Erik Kjeang,^{b*} J. Ledesma-García^a and L. G. Arriaga^{d**}Received (in XXX, XXX) Xth XXXXXXXXX 20XX, Accepted Xth XXXXXXXXX 20XX
DOI: 10.1039/b000000x

The use of three-dimensional flow-through nanoporous electrodes and the merging of a flow-through & air-breathing cathode were explored and successfully applied in a formic acid air-breathing nanofluidic fuel cell. The effects of fuel concentration, reaction stoichiometry and catalyst mass loading were investigated resulting in power densities ranging from 28 to 100 mW cm⁻².

The energy requirements of portable devices and other low power applications have thus far been supplied primarily by batteries. Microfluidic fuel cells have recently been investigated as power sources for these applications due to their potentially high power density.^{1, 2} Among the microfluidic fuel cell technologies being developed, membraneless co-laminar flow cells (CLFC) which use laminar flow dynamics to maintain separation of reactants, have gained considerable attention.^{3, 4} The first of the CLFCs to be demonstrated consisted of two vanadium redox streams flowing over flat deposited electrodes.⁵ Other cells have since been demonstrated using formic acid as fuel and dissolved oxygen as oxidant, with typical power densities between 0.1 to 5 mW cm⁻².^{6, 7} Much greater performance of 26 mW cm⁻² was later demonstrated through the use of an air-breathing cathode⁸ and later improved to 55 mW cm⁻² with a pure oxygen-breathing cathode.^{4, 9} Another concept which has been shown to substantially increase the performance of co-laminar flow cells has been the use of three-dimensional flow-through porous electrodes.¹⁰ It has also recently been shown that higher performance and new functionality can be achieved with higher surface area materials such as nanoporous carbon foam.^{11, 12} The first nanofluidic fuel cell, featuring nanoscale flow of vanadium redox electrolyte within the electrodes combined with a microfluidic cell design, demonstrated vastly enhanced electrochemical kinetics and fuel cell efficiency.¹¹ Although many groups rely on lithography for their cell construction, our group, among others, often uses inexpensive fabrication techniques such as a Control Numerical Computer (CNC) and cutting plotter. Recently, we reported a direct formic acid air breathing microfluidic fuel cell (Figure 1a) where the fuel and the oxidant flow through a flat anode and porous carbon paper as an air breathing cathode obtaining a power density of 29.3 mW cm⁻².¹³ Combining all of the above concepts, the same fabrication technique was used in this work to create a unique

oxygen-breathing cell with nanoporous electrodes focusing on the improvement of power density by combining oxygen from air with a dissolved oxygen solution in a novel low-cost nanofluidic fuel cell which employs a flow-through & air-breathing cathode.

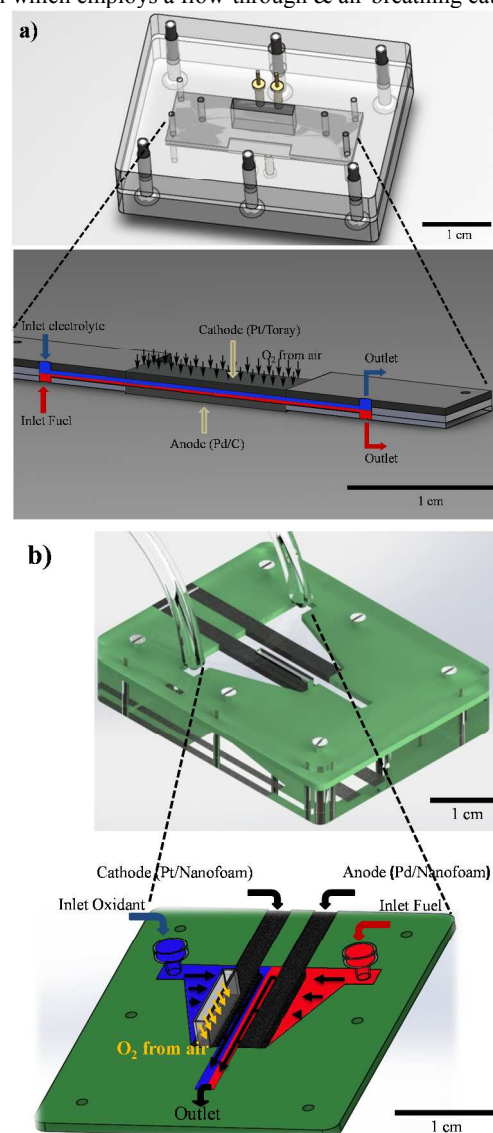


Figure 1 Scheme of a) classic flow-over air breathing microfluidic fuel cell, b) flow-through air breathing nanofluidic fuel cell.

The cell design used in this study is derived from Goulet et al.¹⁴ and is depicted in **Figure 1b** (see SI for a full description of the fabrication procedure). Electrodes were made using commercial carbon nanofoam (Marktech Inc) by spray coating of Pd/C (ETEK, 20% wt) and Pt/C (ETEK, 30% wt) as the anode and cathode electrocatalysts respectively, with a base metal loading of 0.3 mg. The anolyte and the catholyte were prepared using 0.5 M H₂SO₄ as electrolyte. The cathodic stream was bubbled with pure oxygen before entering the cell, where it was combined with oxygen from air in the nanofluidic air-breathing cathode (open window of 0.22 cm², see **Figure S1-d and S3**). The density measurements presented are normalized by the electrode area cross-sectional to the flow of reactants. To avoid ambiguity for three-dimensional electrodes, it has also been recently recommended to use the entire volume of the cell chamber.³ In our device, both cross-sectional area and the entire volume conveniently have almost the same value (0.02 cm² and 0.019 cm³). The flow rates were kept at 100 $\mu\text{L min}^{-1}$ for almost all experiments. In the case of the flow rate effect (2:1, 1:1 and 1:2,) the flow rates were 200:100, 100:100 and 100:200 $\mu\text{L min}^{-1}$ for cathodic/anodic streams, respectively.

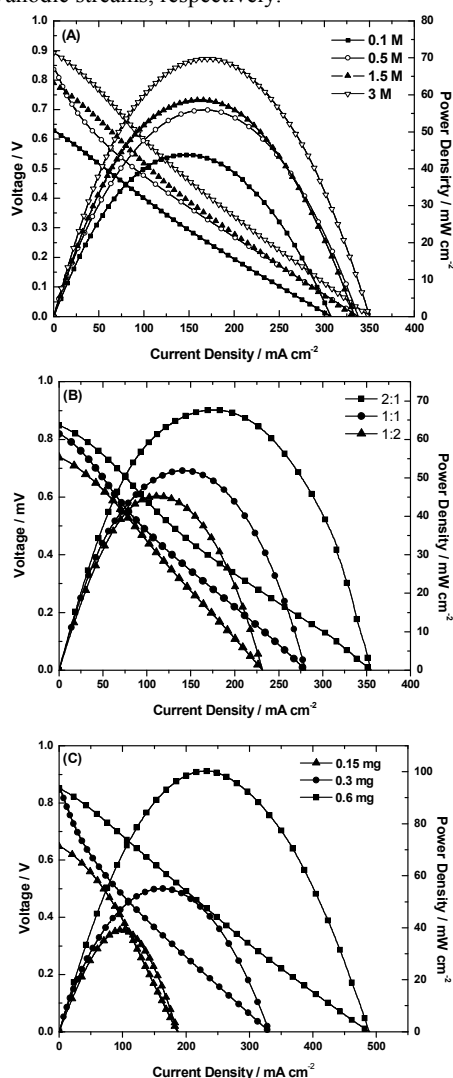


Figure 2 Polarization and power density curves as function of a) the formic acid concentration, b) the flow rate fed in the cathodic and anodic streams (2:1, 1:1 and 1:2), and c) Pd effective metal loading.

Three parameters were investigated in order to evaluate the performance of this new cell: fuel concentration, flow rate and anode Pd metal loading (**Figure 2**). In terms of formic acid concentration (**Figure 2A**), the highest performance was obtained at 3 M: 70 mW cm⁻². The open circuit voltage increased to 0.9 V due to the increase of fuel concentration and also a slightly improvement of the ionic conductivity by increasing the formic acid concentration. Concluding that reactant crossover is reduced with this cell design, as shown by the increasing OCV with increasing fuel concentration (see **Figure S2 and S4**). The flow rate effect (**Figure 2B**) was analyzed using an intermediate concentration of 0.5 M formic acid in order to avoid poisoning the electrode surface. The flow rate was also varied between cathode and anode to understand the limiting behavior of each reactant. The highest power density of 68 mW cm⁻² was obtained with a 2:1 cathode to anode flow rate. This performance was obtained due to an enhancement of the oxygen mass transport. In regards to catalyst loading, the highest performance of 100 mW cm⁻² seen in **Figure 2C** was achieved with three times the base loading (0.6 mg, Pd effective metal loading). This last power density is substantially greater than any previously reported number for a co-laminar cell based on formic acid (see **SI Table S1**) and can be attributed to the combination of customized electrocatalysts on high surface area carbon nanofoam (450 m² g⁻¹) and the addition of both dissolved and gaseous oxygen in the nanofluidic cathode.

Conclusions

In summary, a simple and reliable air breathing nanofluidic fuel cell was built and the concept of flow-through system was merged with an air-breathing cathode. For this novel fuel cell, the power density can be achieved due to the high surface area of carbon nanofoam (450 m² g⁻¹) where the fuel and the oxidant flow through and due to a drastic reduction of the crossover effect because the physical barrier is formed by the reaction by-products instead of the reagents. This and the combination of two sources of oxygen (air and aqueous solution) demonstrated the maximum power density 100 mW cm⁻² reported thus far for membraneless formic acid fuel cells.

Acknowledgements

The authors gratefully acknowledge the financial support through National Council of Science and Technology of Mexico and Natural Sciences and Engineering Research Council of Canada.

Notes and references

- ^a División de Investigación y Posgrado, Facultad de Ingeniería, Universidad Autónoma de Querétaro, 76010 Querétaro, México
- ^b School of Mechatronic Systems Engineering, Simon Fraser University, BC V3T 0A3, Surrey, Canada.
E-mail: *ekjeang@sfu.ca
- ^c Department of Systems Engineering, University of Arkansas, Little Rock, AR 72204, USA
- ^d Centro de Investigación y Desarrollo Tecnológico en Electroquímica, 76703, Querétaro, México.
E-mail: **larriaga@cideteq.mx

† Electronic Supplementary Information (ESI) available: **Figure S1.** Scheme of a) classic flow-over air breathing microfluidic fuel cell, b) flow-through air breathing nanofluidic fuel cell, c) assembled AB-NFC and d) three-dimensional nanoporous electrode and air window dimensions. **Figure S2.** Top view photograph of the nanofluidic fuel cell. Methylene blue was used as colorant at 200 $\mu\text{L min}^{-1}$ flow rate. **Figure S3.** Schematic representation of a) closed and b) open nanofluidic fuel cell. **Figure S4.** Polarization and power density curves of open (NFC) and closed (AB-NFC) nanofluidic fuel cells using 0.5 M formic acid as fuel. **Figure S5.** Stability curve at 0.42 and 0.01 V for 0.5 M formic acid in an AB-NFC. **Table S1.** Current density and power density values for air-breathing formic acid microfluidic fuel cells reported in the literature compared to the present results. See DOI: 10.1039/b000000x/

1. C. K. Dyer, *J. Power Sources*, 2002, **106**, 31-34.
2. S. Pennathur, J. C. T. Eijkel and A. Van der Berg, *Lab Chip*, 2007, **7**, 1234-1237.
3. M.-A. Goulet and E. Kjeang, *J. Power Sources*, 2014, **260**, 186-196.
4. E. Kjeang, *Microfluidic Fuel Cells and Batteries*, Springer International Publishing, 2014.
5. R. Ferrigno, A. D. Stroock, T. D. Clark, M. Mayer and G. M. Whitesides, *J. Am. Chem. Soc.*, 2002, **124**, 12930-12931.
6. E. Kjeang, D. Djilali and D. Sinton, *J. Power Sources*, 2009, **186**, 353-369.
7. A. D  ctor, J. P. Esquivel, M. J. Gonz  lez, M. Guerra-Balc  zar, J. Ledesma-Garc  a, N. Sabat   and L. G. Arriaga, *Electrochim. Acta*, 2013, **92**, 31-35.
8. R. S. Jayashree, L. Ganes, E. R. Choban, A. Primak, D. Natarajan, L. J. Markoski and P. J. A. Kenis, *J. Am. Chem. Soc.*, 2005, **127**, 16758-16759.
9. R. S. Jayashree, S. K. Yoon, F. R. Brushett, P. O. Lopez-Montesinos, D. Natarajan, L. J. Markoski and P. J. A. Kenis, *J. Power Sources*, 2010, **195**, 3569-3578.
10. E. Kjeang, R. Michel, D. A. Harrington, D. Djilali and D. Sinton, *J. Am. Chem. Soc.*, 2008, **130**, 4000-4006.
11. J. W. Lee and E. Kjeang, *J. Power Sources*, 2013, **242**, 472-477.
12. J. W. Lee, M.-A. Goulet and E. Kjeang, *Lab Chip*, 2013, **13**, 2504-2507.
13. A. Moreno-Zuria, A. D  ctor, F. M. Cuevas, J. P. Esquivel, N. Sabat  , J. Ledesma-Garc  a, L. G. Arriaga and A. U. Ch  vez-Ram  rez, *J. Power Sources*, 2014, **269**, 783-788.
14. M.-A. Goulet and E. Kjeang, *Electrochim. Acta*, 2014, DOI: 10.1016/j.electacta.2014.1003.1092.